

Synthesis, Photophysical and Electrophosphorescent Properties of Fluorene-Based Platinum(II) Complexes

Mai-Yan Yuen, Steven C. F. Kui, Kam-Hung Low, Chi-Chung Kwok, Stephen Sin-Yin Chui, Chun-Wah Ma, Nianyong Zhu, and Chi-Ming Che*^[a]

Abstract: A series of platinum(II) complexes bearing tridentate cyclometalated C[^]N[^]N (C[^]N[^]N=6-phenyl-2,2'-bipyridine and π -extended R-C[^]N[^]N=3-[6'-(naphthalen-2''-yl)pyridin-2'-yl]-isoquinoline) ligands with fluorene units have been synthesised and their photophysical properties have been studied. The fluorene units are incorporated into the cyclometalated ligands by a Suzuki coupling reaction. An increase in the π -conjugation of the cyclometalated ligands confers favourable photophysical properties compared to the 6-phenyl-2,2'-bipyridine analogues. The fluorene-based platinum(II) complexes display vibronic-

structured emission bands with λ_{\max} = 558–601 nm, and high emission quantum yields up to 0.76 in degassed dichloromethane. Their emissions are tentatively assigned to excited states with mixed ³IL/³MLCT parentage (IL=intraligand, MLCT=metal-to-ligand charge transfer). The crystal structures of these platinum(II) complexes reveal extensive Pt^{II}... π and/or π - π interactions. The fluorene-based

Keywords: charge transfer • cyclometalation • electrophosphorescence • fluorenes • organic light-emitting diodes • platinum

platinum(II) complexes are soluble in organic solvents, have high thermal stability with decomposition temperature >350°C, and can be thermally vacuum-sublimed or solution-processed as phosphorescent dopants for the fabrication of organic light-emitting diodes (OLEDs). A monochromatic OLED with **3d** as dopant (2 wt %) fabricated by vacuum deposition gave a current efficiency of 14.7 cd A⁻¹ and maximum brightness of 27000 cd m⁻². A high current efficiency (9.2 cd A⁻¹) has been achieved in a solution-processed OLED using complex **3f** (5 wt %) doped in a PVK (poly(9-vinyl-carbazole)) host.

Introduction

Since the first report on organic light-emitting diodes (OLEDs) by Tang,^[1] the quest for new electroluminescent materials has become a main focus in materials science.^[2] Although significant advances have been made in the design and fabrication of high performance OLEDs,^[3] the fabrication of OLEDs by vacuum deposition is costly. Conjugated polymers and oligomers have been studied extensively as so-

lution-processable light-emitting materials for polymer light-emitting diodes (PLEDs),^[4] due to the low fabrication cost for large-area displays through spin-coating, inkjet-printing, or spray-coating techniques.^[5] Recently, several groups have reported efficient phosphorescent or fluorescent OLEDs prepared by spin-coating solutions of small organic molecules^[6] or iridium(III) complexes.^[7] The blending of small molecules into the polymer host offers an alternative route for solution-processed OLEDs. However, the differences in both entropy and enthalpy values between the polymer and the small molecules in the polymer blend may result in phase separation, which leads to the formation of traps for charge carriers. In addition, the HOMOs and LUMOs of the polymer host are different from those of the small molecules, leading to incomplete energy transfer from host to dopant. Therefore, there has been considerable interest in the design of emissive small molecules which are suitable for blending with the polymer host.

π -Conjugated organic oligomers coordinated to transition-metal ions have emerged as a new class of molecular electronic materials.^[7] In particular, oligomeric organic li-

[a] Dr. M.-Y. Yuen, Dr. S. C. F. Kui, Dr. K.-H. Low, Dr. C.-C. Kwok, Dr. S. S.-Y. Chui, C.-W. Ma, N. Zhu, Prof. C.-M. Che
Department of Chemistry
Institute of Molecular Functional Materials
HKU-CAS Joint Laboratory on New Materials
and State Key Laboratory on Synthetic Chemistry
The University of Hong Kong
Pokfulam Road, Hong Kong (China)
Fax: (+852)2915-5176
E-mail: cmche@hku.hk

Supporting information for this article is available on the WWW under <http://dx.doi.org/10.1002/chem.201001570>.

gands coordinated to heavy metal ions are of importance, as they can be utilised as solution-processing phosphorescent materials.^[8] Because intersystem crossing (ISC) becomes efficient as a result of spin-orbit coupling, emission from both singlet and triplet states can be harvested, and 100% internal quantum efficiency (IQE) can, in principle, be achieved. Using phosphorescent transition-metal complexes as light-emitting materials, a number of cyclometalated iridium(III) complexes of 2-phenylpyridine have been studied as dopants in polymeric light-emitting devices.^[9] In contrast, there have been no literature reports on utilising phosphorescent cyclometalated platinum(II) complexes as molecular dopants for either vacuum-deposited OLEDs or solution-processed PLEDs. Square-planar d⁸ cyclometalated platinum(II) complexes have attracted much attention as phosphorescent dopant materials.^[2b] Among them, platinum(II) complexes containing aromatic N-donor and/or cyclometalated ligands are known to display a variety of emissive excited states,^[10] including ligand-field (LF), metal-to-ligand charge transfer (MLCT), intraligand (IL) $\pi \rightarrow \pi^*$, excimeric and oligomeric metal-metal-to-ligand charge-transfer (MMLCT) states. The relative energy of these excited states can be tuned by varying the ligands coordinated to the Pt^{II} ion.

We are attracted to the prospect of incorporating fluorene units in the design of cyclometalated platinum(II) complexes. Previous studies have revealed that, by increasing the π -conjugation of cyclometalated ligands, the structural distortion of the triplet excited state is minimised, resulting in an enhancement of the phosphorescence quantum yield.^[11] Whereas there are many reports on fluorene-based iridium(III) complexes,^[9] there are only a few studies on luminescent platinum(II) complexes containing ligands with fluorene units.^[12] We envisage that by connecting fluorene units to cyclometalated C[^]N[^]N ligands, the high emission quantum yields of the Pt(C[^]N[^]N) complexes could be retained, and their solubility in common organic solvents could be improved.^[13] The fluorene-based platinum(II) complexes could easily be blended with the polymer host to produce morphologically stable thin films through ink-jet printing or spin coating. Very recently, Shao et al. reported the photophysical and nonlinear optical properties of platinum(II) complexes of 6-phenyl-4-(9,9-dihexylfluorene-2-yl)-2,2'-bipyridine.^[12] Herein we describe the synthesis, crystal structures and photophysical properties of platinum(II) complexes containing fluorene unit(s) incorporated into the cyclometalated 6-phenyl-2,2'-bipyridine (C[^]N[^]N complex types **1** and **2**) or 3-[6'-(naphthalen-2''-yl)pyridin-2'-yl]isoquinoline ligands (R-C[^]N[^]N complex types **3–6**). Complexes **3a**, **3d**, **3f**, **3g**, **5b**, **5c** and **6c** (Scheme 1) have been tested for the fabrication of vacuum-sublimated and solution-processed OLEDs.

Results and Discussion

Synthesis and characterisation: Fluorene units are incorporated in the periphery of C[^]N[^]N (Types **1** and **2**) and π -ex-

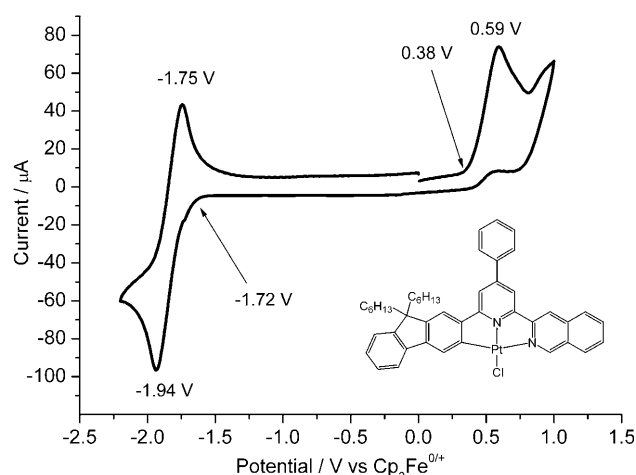
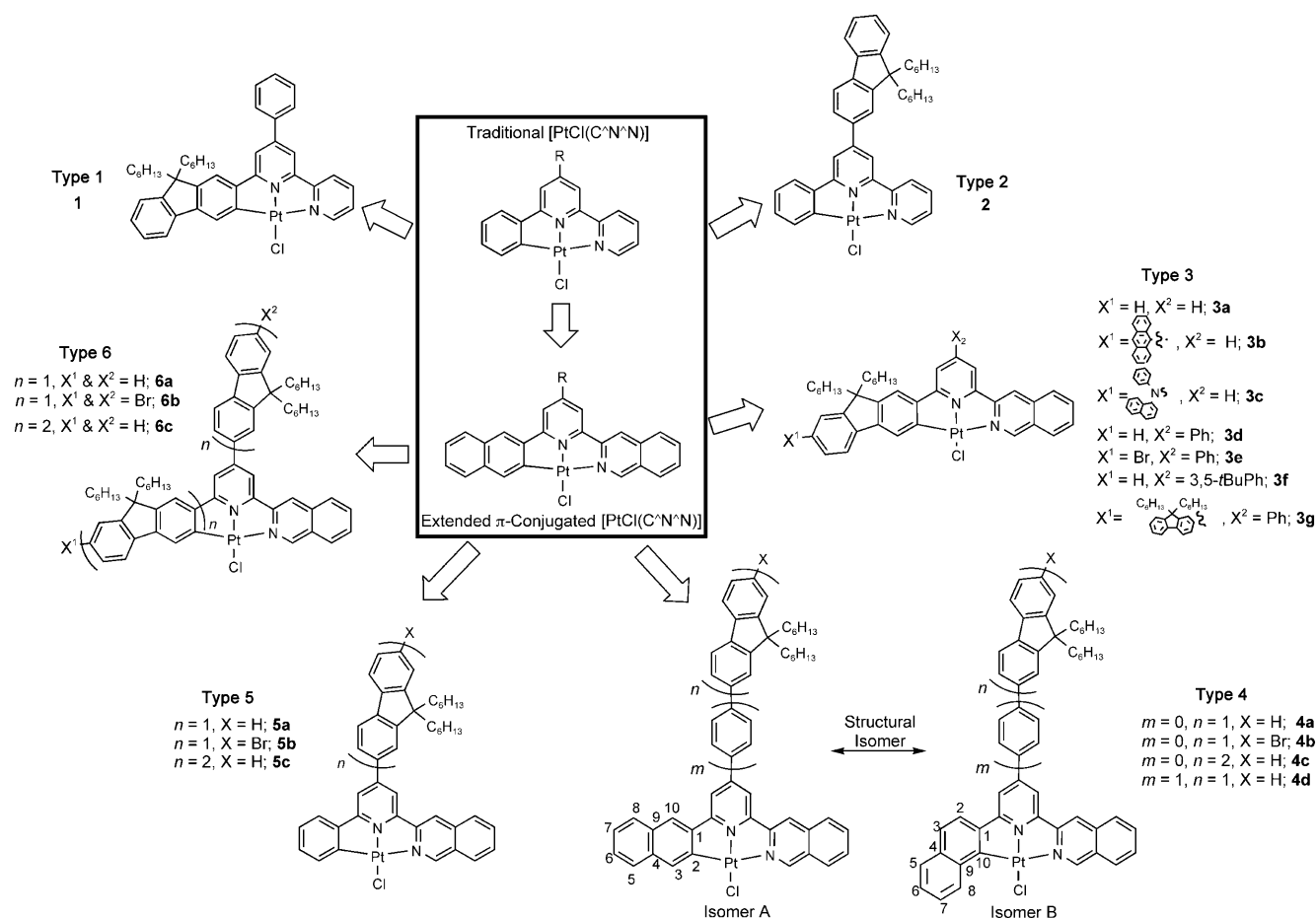


Figure 1. Cyclic voltammogram of complex **3d** in DMF.

tended R-C[^]N[^]N (Types **3–6**) ligands. The cyclometalated ligands were prepared according to literature procedures,^[11a] comprising several steps involving: 1) alkylation of the methylene (fluorene) motif; 2) bromination; 3) acetylation, 4) Suzuki coupling for the synthesis of fluorene units; and 5) formation of cyclometalated (C[^]N[^]N) ligands. In all cases, the C[^]N[^]N ligand is connected to the 2- and/or 2,7-positions of the fluorene unit(s) (Scheme 1). The experimental procedures and characterisation data of the ligands and starting materials are given in the Supporting Information. The platinum(II) complexes were obtained in high yields by heating K₂PtCl₄ under reflux with the corresponding ligands in a mixture of glacial acetic acid and CHCl₃ (v:v, 10:1). Compared to other cyclometalated Pt^{II} complexes, the fluorene-based cyclometalated Pt^{II} complexes exhibit better solubility in common organic solvents, including toluene and chlorobenzene. This is important for applications involving ink-jet printing, spin coating and blending with a polymer host for solution-processed OLEDs. Each ligand and corresponding platinum(II) complex have been characterised by ¹H, ¹H-¹H COSY and NOESY NMR spectroscopy, EIMS or fast-atom bombardment (FAB) (+ve) mass spectrometry and elemental analyses. The ¹H NMR spectra of **1**, **2**, **3a**, **5a** and **6a** together with proton assignments are depicted as representative examples in Figures S5–S9 of the Supporting Information.

The ¹H NMR spectra of the as-prepared complexes **4a–d** (Supporting Information, Figures S10–S14) revealed two species with approximately 1:1 molar ratio in each of the cases examined. Further investigation through 2D NMR (¹H-¹H COSY and NOESY) and ¹⁹⁵Pt NMR experiments confirmed two isomeric forms generated in the course of the reactions between K₂PtCl₄ and the fluorene-based cyclometalated ligands (Figure 1, Type **4**). For complexes **4a–d**, the platinum(II) ion is coordinated by the π -extended R-C[^]N[^]N ligand through the C2 or C10 atom, giving rise to the linear form (Pt...C2, Isomer A) or bent form (Pt...C10, Isomer B) (Scheme 1). The Pt...C10 coordination (Isomer B) causes the C8 and H8 atoms to be in close proximity to



Scheme 1. Evolutional scheme of fluorene-based platinum(II) complexes.

the platinum(II) ion, thus, there is a shift of the ^1H NMR signal of H8 to the downfield region (**4a**: 9.62 ppm in CD_2Cl_2 ; **4b**: 10.03 ppm in d_7 -DMF; **4c**: 9.48 ppm in CD_2Cl_2 and **4d**: 9.36 ppm in CD_2Cl_2) (Figures S10–S14). The structure of isomeric form A of **4c** has been revealed by X-ray crystal analysis (Figures S29 and S30). The problem of structural isomerism can be avoided by changing the ligand from 3-(6'-(naphthalen-2'-yl)pyridin-2'-yl)isoquinoline (Type 4) to 3-(6'-phenylpyridin-2'-yl)isoquinoline (Type 5).

Thermogravimetric analysis (TGA) of the cyclometalated platinum(II) complexes was performed, and the data are summarised in Table 1. The decomposition temperatures of all of the complexes (384–473 °C)

Table 1. Summary of electrochemical data and decomposition temperature for complexes **1**, **2**, **3a–g**, **4a–d**, **5a–c** and **6a–c**.

	E_{red} [V] ^[a]		E_{ox} [V] ^[a]		HOMO [eV] ^[b]	LUMO [eV] ^[b]	Electrochemical bandgap [eV]	T_d [°C]
	onset	$E_{1/2}$	onset	E_{peak}				
1	−1.62	−1.73	0.27	0.60	−5.07	−3.18	1.89	451
2	−1.60	−1.71	0.36	0.47	−5.16	−3.20	1.96	448
3a	−1.80	−1.89	0.43	0.68	−5.23	−3.00	2.23	433
3b	−1.77	−1.85	–	–	n/a ^[c]	−3.03	n/a ^[c]	463
3c	−1.79	−1.91	0.30	0.51	−5.10	−3.01	2.09	436
3d	−1.72	−1.85	0.38	0.59	−5.18	−3.08	2.10	448
3e	−1.72	−1.84	0.30	0.51	−5.10	−3.08	2.02	443
3f	−1.77	−1.88	0.44	0.62	−5.24	−3.03	2.21	466
3g	−1.71	−1.82	0.39	0.56	−5.19	−3.09	2.10	451
4a	−1.70	−1.81	0.35	0.61	−5.15	−3.10	2.05	452
4b	−1.68	−1.80	0.30	0.58	−5.10	−3.12	1.98	384
4c	−1.68	−1.78	0.32	0.54	−5.12	−3.12	2.00	448
4d	−1.71	−1.81	0.34	0.63	−5.14	−3.09	2.05	427
5a	−1.71	−1.83	0.34	0.48	−5.14	−3.09	2.05	444
5b	−1.71	−1.79	0.32	0.52	−5.12	−3.09	2.03	419
5c	−1.68	−1.80	0.36	0.59	−5.16	−3.12	2.04	473
6a	−1.71	−1.83	0.44	0.56	−5.24	−3.09	2.15	438
6b	−1.66	−1.77	0.37	0.53	−5.17	−3.14	2.03	392
6c	−1.72	−1.80	0.36	0.55	−5.16	−3.08	2.08	419

[a] Determined in DMF at 298 K with 0.1 M $n\text{Bu}_4\text{NPF}_6$ as supporting electrolyte; scanning rate: 50 mV s^{−1}; values are versus $\text{Cp}_2\text{Fe}^{0+}$. [b] The HOMO and LUMO level were calculated from onset potentials using $\text{Cp}_2\text{Fe}^{0+}$ values of 4.8 eV below the vacuum level.^[14] [c] n/a = not applicable.

are comparable to those of previously reported cyclometalated [PtCl(π -extended R-C^{^N^N})]^[11a] and [PtCl(O^{^N^N})] complexes^[15] (H-O^{^N^N}=2-(6'-(pyridin-2'-yl)pyridine-2'-yl)phenol). The cyclic voltammograms of complexes **1**, **2**, **3a-g**, **4a-d**, **5a-c** and **6a-c** in DMF (0.1 mol dm⁻³ *n*Bu₄NPF₆) reveal one quasi-reversible reduction couple with $E_{1/2}$ at -1.71 to -1.91 V vs. $E_{1/2}$ of the Cp₂Fe^{0/+} couple and an irreversible oxidation wave at 0.47 to 0.68 V. The electrochemical data are summarised in Table 1. Complex **3b** shows no oxidation wave within the electrochemical window of the DMF solvent. With reference to previously reported cyclometalated platinum(II) complexes of C^{^N^N} ligands,^[10-12] the reduction couple is assigned to the ligand-centred reduction of the fluorene-based C^{^N^N} ligand. The reduction potentials of complexes **1** and **2** (\approx -1.7 V) are less cathodic than those of related cyclometalated platinum(II) complexes containing extended π -conjugated R-

C^{^N^N} ligands (complexes **3a-g**, **4a-d**, **5a-c** and **6a-c**, which range from -1.77 to -1.91 V). Comparison of the reduction potentials among the different types (Types **3-6**) of fluorene-based [Pt-(C^{^N^N})] complexes reveals that the $E_{1/2}$ of the reduction couple is less sensitive to the number of fluorene units.

X-ray crystallography: Crystallographic data of **2**, **3a**, **3d** and **4c**, intermolecular π - π and Pt...Pt distances, and selected bond lengths and angles are given in the Supporting Information.^[16] Perspective views and crystal-packing diagrams of **2**, **3a** and **3d** are depicted in Figure 2, and those for **4c** are given in the Supporting Information (Figure S29). The coordination geometries of complexes **2**, **3a**, **3d** and **4c** are similar to those of [PtCl(C^{^N^N})]^[10a] and [PtCl(π -extended R-C^{^N^N})]^[11a]. In each of the complexes, the Pt ion adopts a distorted square-planar geometry, as revealed by the N-

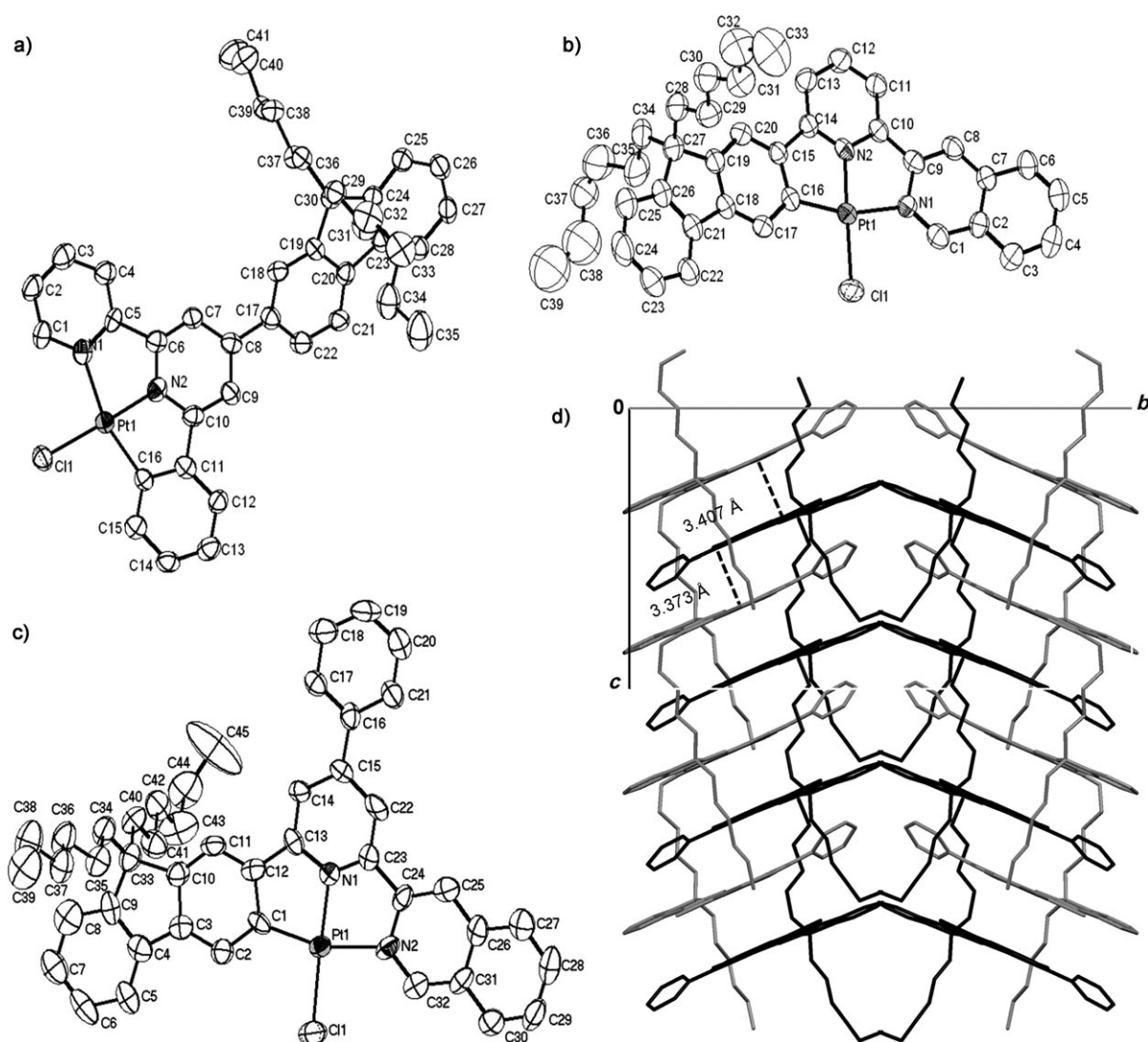


Figure 2. Perspective views of a) **2**, b) **3a**, c) **3d** and d) molecular packing diagram of **3d** highlighting the π - π interactions between the molecules (the two crystallographically inequivalent molecules are represented in black and grey).

Pt–C angles of 161.49° (**2**), 162.10° (**3a**), 162.10° (**3d**) and 158.07° (**4c**), all of which deviate significantly from the ideal value of 180°. The Pt–N_{pyridine} and Pt–N_{isoquinoline} (**3a**, **3d** and **4c**) or Pt–N_{pyridine} (**2**) distances of the complexes are similar (Pt–N_{pyridine}: 1.942–1.969 Å; Pt–N_{isoquinoline}/Pt–N_{pyridine}: 2.051–2.102 Å) and are comparable to those of previously reported [PtCl(R-C[^]N[^]N)]^[10,11] complexes. The Pt–C distances of **3a** (1.974 Å) and **3d** (1.969 Å) are slightly shorter, and the platinum(II) ion in each case is ligated by the deprotonated carbon atom (C⁻) of the fluorene unit. In their crystal structures, complexes **2**, **3a** and **4c** are packed in a head-to-tail fashion, with substantial π overlap of the fluorene-based C[^]N[^]N ligands. The interplanar distances between two [Pt-(C[^]N[^]N)] moieties are in the range of 3.28–3.40 Å, revealing the presence of π – π interactions. In all of these cases, the shortest Pt··Pt distances between the molecules are >4 Å, revealing no Pt··Pt interactions.

The crystal structure of **3d** consists of two crystallographically inequivalent molecules per asymmetric unit (Figure S27, denoted by Pt1 and Pt2). In contrast to **2**, **3a** and **4c**, in which the molecules in each case are packed as head-to-tail dimers, two molecules of **3d** are staggered with a torsional angle N_{pyridine}–Pt–Pt–N_{pyridine} of 127.2°. Extensive intermolecular π – π interactions align the molecules into a 1D column with alternate interplanar distances of 3.373–3.395 Å (Figure 2d). One salient feature is the presence of Pt·· π interactions between the staggered molecules, with a Pt··C_{C[^]N[^]N}} distance of 3.407 Å.

Small single crystals of **4c** were obtained by slow cooling of saturated solution of **4c** in hot DMF. The X-ray diffraction data collected at 100 K are of sufficient quality for locating the fluorene-based C[^]N[^]N ligand and the Pt and Cl atoms, but are not good enough for the identification of the exact location and orientation of the *n*-hexyl chains. The solution of the X-ray crystal structure using this set of X-ray diffraction data revealed isomer A (linear form; coordination through Pt··C2) for **4c**; molecules of **4c** are packed as dimers in a head-to-tail fashion, with an interplanar distance of 3.371 Å (Figure S30).

Photophysical properties: The UV/Vis absorption spectra of complexes **1**, **2**, **3a–g**, **4a–d**, **5a–c** and **6a–c** in dichloromethane at 298 K exhibit an intense vibronic-structured absorption band, with peak maxima at 310–350 nm, ϵ values of 10⁴–10⁵ dm³ mol⁻¹ cm⁻¹, and a moderately intense absorption shoulder at 400–420 nm (Table 2). The absorption λ_{\max} values resemble those of other cyclometalated C[^]N[^]N platinum(II) complexes,^[10–12,15] but with increased absorption extinction coefficients. The photophysical data of **1**, **2**, **3a–g**, **4a–d**, **5a–c** and **6a–c** are summarised in Table 1, and the corresponding electronic absorption spectra are depicted in Figure 3 and Figures S32–S40. As revealed in Figure 3, the intense absorption bands in the UV region (310–350 nm) are derived from intraligand (IL) $\pi \rightarrow \pi^*$ transitions of the fluorene-based C[^]N[^]N ligands, because similar transitions are also present in the free ligands (Figure S31). The cyclometalated ligands containing fluorene units display vibronic-

structured absorption bands at 325–355 nm, the absorption maximum of which is red-shifted with an increasing number of fluorene units. The molar extinction coefficient (ϵ) of the free ligand also increases with an increasing number of fluorene units incorporated, consistent with an increase in π -conjugation. A similar red shift and increase in molar extinction coefficient have also been observed in the absorption spectra of the corresponding platinum(II) complexes. For complexes **1** and **2** containing the related 6-phenyl-2,2'-bipyridine (C[^]N[^]N) ligand, the extinction coefficients (ϵ) in the UV region are substantially lower than those of other complexes containing the π -extended C[^]N[^]N ligands. With reference to other related platinum(II) complexes,^[10–12,15] the moderately intense bands at 400–420 nm are tentatively assigned to the electronic transitions with mixed ¹MLCT/³IL characters. Similar electronic absorption spectra were reported by Shao et al. in the study of platinum(II) complexes of 6-phenyl-4-(9,9-dihexylfluoren-2-yl)-2,2'-bipyridine.^[12] The effect of solvent polarity on the UV/Vis absorption spectra of **3a** (Figure S39) and **6a** (Figure 4) has been investigated. The low-energy absorption band λ_{\max} of **3a** is blue-shifted with increasing solvent polarity: 433 nm in toluene; 431 nm in CH₂Cl₂; 431 nm in ethyl acetate; and 426 nm in DMF. Likewise, the low-energy absorption peak maximum of **6a** displays a similar shift (λ_{\max}): 450 nm in toluene; 442 nm in CH₂Cl₂; 428 nm in ethyl acetate; 418 nm in CH₃CN; and 417 nm in DMF. Such a blue shift in the absorption energy suggests that the polarity of the ground state is higher than that of the excited state; similar features have been observed in other cyclometalated platinum(II) complexes.^[10,11,15]

Complexes **1**, **2**, **3a–g**, **4a–d**, **5a–c** and **6a–c** are strongly emissive, with emission quantum yields (Φ) up to 0.73 in degassed dichloromethane at 298 K. The emission lifetimes (τ) of the complexes are in the microsecond time regime, suggesting that the emission in each case originates from the triplet excited state. Complexes **1** and **2** display a structureless emission band at λ_{\max} = 588 and 568 nm, respectively, and with emission quantum yields of 0.16 and 0.07, respectively, both of which are substantially higher than that of the [PtCl(C[^]N[^]N)] complex (λ_{\max} = 565 nm, Φ = 0.025).^[10a] The emission spectra and excited-state lifetimes for complexes **1** and **2** are similar to those of the platinum(II) complexes with fluorenyl-substituted C[^]N[^]N ligands recently reported by Shao et al.^[12] One point worth addressing is the effect of the fluorene substitution on the emission wavelength and quantum yield of complexes **1** and **2**. By incorporating a fluorenyl C donor to give the cyclometalated 6-[(9,9-dihexylfluoren-2-yl)pyridin-2-yl]isoquinoline ligand, the emission λ_{\max} is red-shifted from 563 nm in **3a** to 588 nm in **3g** with increased emission quantum yield. This phenomenon is attributed to the stronger σ -donor properties of the fluorenyl carbanion C donor compared to the aryl carbanion C donor; the former subsequently raises the $d\sigma^*$ of the Pt^{II} ion and increases the energy gap between the MLCT and non-emissive d–d states. More importantly, the emission quantum yield is further increased to 0.73 (**3d**) when the pyridine

Table 2. Photophysical data of complexes **1**, **2**, **3a–g**, **4a–d**, **5a–c** and **6a–c**.

	UV/Vis absorption ^[a] λ_{max} [nm] (ϵ [mol ⁻¹ dm ⁻³ cm ⁻¹])	Solution ^[a] λ_{max} [nm] (τ [μ s])	Quantum yield $\phi^{\text{[b]}}$	Photoluminescence Data		
				Solid state, 298 K λ_{max} [nm] (τ [μ s])	Solid state, 77 K λ_{max} [nm] (τ [μ s])	Glassy solution, 77 K ^[c] λ_{max} [nm] (τ [μ s])
1	294 (14300), 311 (14200), 330 (13900), 376 (9800), 445 (2000)	588 (2.2)	0.16	587 (3.1), 626 (2.9)	587 (21.2), 638 (19.7)	556 (31.7), 603 (31.1)
2	216 (144600), 281 (30337), 330 (22800), 352 (25400), 432 (7320)	568 (1.0)	0.07	604 (0.1)	558 (8.0), 625 (8.0), 670 (6.3)	558 (22.8), 603 (21.7), 664 (21.1)
3a	243 (43800), 284 (21400), 314 (38400), 349 (40400), 382 (17000), 418 (sh, 5600)	563 (9.1)	0.35	563 (3.1), 604 (3.0), 660 (1.2)	561 (4.1), 607 (3.9), 661 (1.2)	553 (26.5), 575 (21.4), 600 (21.2), 650 (18.4)
3b	316 (28800), 356 (34500), 383 (23400), 409 (95400), 446 (sh, 2480)	566 (4.3)	0.07	584 (2.6), 617 (2.5), 672 (1.7)	580 (6.1), 633 (5.7), 694 (5.2)	560 (20.8), 608(20.4), 659 (19.7)
3c	302 (18900), 341 (16200), 390 (18900), 471 (sh, 4960)	601 (3.3)	0.02	594 (1.2), 639 (1.2), 688 (1.1)	594 (5.4), 643 (5.2), 709 (4.2)	594 (10.9), 634 (9.3), 693 (8.9)
3d	319 (48700), 350 (41000), 387 (19100), 418 (8040)	568 (2.6), 611 (2.5), 668 (2.5)	0.73	572 (1.2), 611 (1.1), 670 (0.6)	570 (4.3), 620 (3.7), 673 (3.4)	560 (11.2), 609 (10.5), 673 (10.3)
3e	322 (39300), 351 (32100), 387 (15600), 422 (6210)	568 (3.6)	0.23	587 (1.2)	580 (5.6), 630 (5.1), 691 (3.7)	564 (9.3), 610 (9.1), 666 (8.4)
3f	327 (42200), 355 (33200), 430 (6700)	568 (9.8), 609 (7.8), 666 (5.6)	0.73	564 (3.2), 608 (2.9), 666 (2.2)	565 (7.3), 608 (7.2), 666 (5.0)	557 (15.3), 601 (13.5), 654 (11.8)
3g	306 (43500), 346 (41800), 411 (21800), 482 (3500)	588 (7.6), 604 (5.9)	0.10	588 (2.3), 674 (1.9)	594 (3.3), 640 (2.8), 709 (2.6)	579 (13.6), 628 (12.8), 685 (11.9)
4a	286 (38200), 342 (51200), 399 (15800), 420 (12600), 469 (sh, 2020)	603 (8.7), 658 (8.0)	0.18	619 (8.8), 671 (6.9)	619 (12.5), 673 (10.1)	560 (55.8), 601 (51.2), 665 (44.8)
4b	290 (37600), 342 (53200), 397 (16100), 424 (11700), 465 (sh, 1920)	603 (7.6)	0.12	627 (4.2), 677 (2.9)	625 (11.6), 678 (11.1)	542 (28.8), 590 (26.1), 638 (22.9)
4c	316 (87400), 348 (98600), 379 (85000), 423 (45600), 472 (sh, 3230)	568 (6.2), 603 (5.1)	0.46	604 (5.8), 625 (5.0)	606 (11.8), 667 (11.3)	563 (26.4), 597 (26.2), 647 (20.18)
4d	342 (54300), 352 (58800), 418 (12000), 453 (sh, 2310)	604 (7.3), 656 (7.0)	0.22	621 (4.3), 662 (4.2)	594 (11.0), 659 (11.0), 699 (9.8)	582 (58.8), 633 (53.3)
5a	249 (38900), 291 (24200), 3454 (32100), 421 (7900), 449 (1480)	558 (13.2), 598 (12.9), 665 (12.5)	0.47	554 (0.3), 582 (0.2)	558 (6.0), 600 (5.4), 661 (3.8)	548 (20.1), 591 (19.8), 641 (18.2)
5b	292 (29600), 346 (39300), 422 (10100), 473 (sh, 2430)	561 (12.6), 605 (12.3), 674 (11.8)	0.26	559 (0.7), 605 (0.7)	569 (5.8), 618 (9.4), 673 (8.5)	547 (25.6), 589 (25.4), 638 (18.9)
5c	253 (41600), 303 (33300), 329 (38600), 373 (35900), 426 (16500), 483 (sh, 2070)	570 (22.9), 616 (22.1), 676 (19.8)	0.34	551 (0.1), 594 (0.1), 666 (0.1)	566 (5.5), 609 (6.0), 674 (8.5)	568 (46.7), 606 (40.3), 671 (34.7)
6a	252 (127900), 343 (64900), 388 (25100), 420 (16000), 442 (10900), 472 (sh, 2350)	572 (9.9), 612 (9.8), 673 (9.5)	0.33	571 (0.1), 617 (0.1), 673 (0.1)	575 (5.3), 662 (5.2), 676 (4.8)	562 (28.1), 609 (28.0), 667 (28.0)
6b	257 (52000), 349 (73200), 424 (15500), 463 (2880)	570 (9.0), 614 (8.8), 675 (8.5)	0.32	576 (1.3), 621 (1.2), 682 (1.1)	592 (9.4), 635 (9.4), 692 (6.3)	563 (15.4), 612 (12.6), 668 (11.3)
6c	253 (56900), 335 (70800), 375 (86400), 468 (4680)	586 (12.1), 631 (11.6)	0.36	583 (0.8), 533 (0.8), 687 (0.6)	591 (5.7), 637 (4.0), 696 (3.8)	584 (32.1), 631 (32.0), 681 (30.2)

[a] Determined in degassed dichloromethane solution. [b] Absolute emission quantum yield was measured by the optical dilute method with [Ru(bpy)₃]Cl₂ (bpy = 2,2'-bipyridine) in degassed acetonitrile as standard ($\phi_r = 0.062$) and calculated by: $\phi_s = \phi_r (B_r/B_s)(n_s/n_r)^2 (D_s/D_r)$, in which the subscripts s and r refer to sample and reference standard solution respectively, n is the refractive index of the solvents, D is the integrated intensity and ϕ is the luminescence quantum yield. The excitation intensity B is calculated by: $B = 1 - 10^{-AL}$, in which A is the absorbance at the excitation wavelength and L is the optical path length ($L = 1$ cm in all cases). The refractive indices of the solvents at room temperature were taken from standard sources. Errors for ϕ values ($\pm 10\%$) are estimated. [c] In DMF: MeOH: EtOH mixture ($v:v:v = 1:1:4$).

ring in C^{^N^N} is replaced by isoquinoline. A previous study on structurally related [PtCl(π -extended R-C^{^N^N})] complexes (π -extended (R-C^{^N^N}) = 3-(6'-(naphthalen-2''-yl)pyridin-2'-yl)isoquinoline) using DFT calculations^[11b] revealed that the isoquinoline ring increases the π -conjugation of the cyclometalated ligand. This extended π -conjugation leads to a destabilisation of the HOMO d_{xz} (Pt) orbital, consequently removing the degeneracy of the d_{xz} and d_{xy} orbitals. Thus, the [PtCl(R-C^{^N^N})] complexes (R-C^{^N^N} = extended π -conjugated cyclometalated ligands) do not undergo excited-state Jahn–Teller distortion and the C^{^N^N}-Pt-Cl plane remains coplanar upon excitation, resulting in the enhancement of the emission quantum yield.^[11b] Complexes **1**, **2**, **3a–g**, **4a–d**, **5a–c** and **6a–c** display vibronic-structured emissions with $\lambda_{\text{max}} = 558$ –604 nm and with vi-

bronic progression ≈ 1300 cm⁻¹, which are characteristic of the C=C and C=N stretching frequencies of the fluorene unit and the C^{^N^N} ligand. This indicates the involvement of the fluorene-based cyclometalated ligand in the excited state. We found that the emission energies of **3a** and **6a** are only slightly affected by solvent polarity. The emission maximum is blue-shifted from 567 nm (in toluene) to 563 nm (CH₂Cl₂), 561 nm (ethyl acetate) and 559 nm (DMF) for **3a** and from 576 nm (toluene) to 572 nm (CH₂Cl₂), 570 nm (ethyl acetate), 567 nm (CH₃CN) and 566 nm (DMF) for **6a** (Figure S40). The vibronic-structured emission in solution at room temperature is consistent with the mixing of intraligand (IL) ³ $\pi \rightarrow \pi^*$ character in the ³MLCT excited states. With reference to previous studies,^[11a] we tentatively assign the solution emission to mixed ³IL/³MLCT excited states.

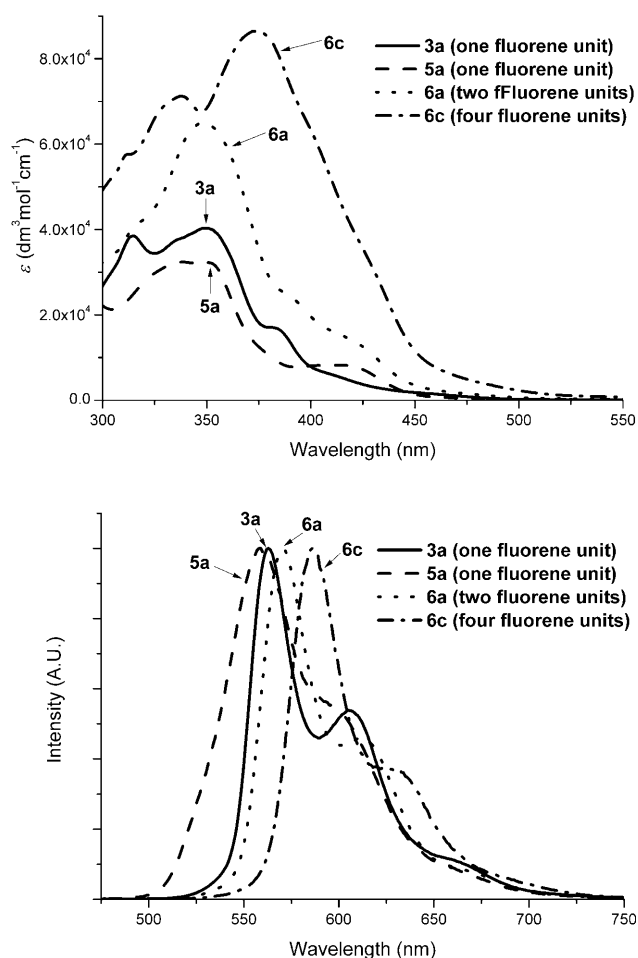


Figure 3. UV/Vis absorption (top) and emission (bottom) spectra of cyclometalated platinum(II) complexes containing fluorene unit(s).

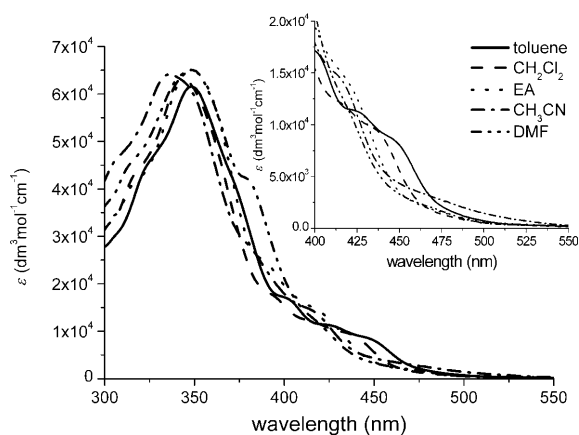


Figure 4. UV/Vis absorption spectra of **6a** in different solvents.

There is a small red shift in the emission λ_{max} along the series: complexes **5a** (one fluorene) to **5c** (two fluorene units) from 558 to 570 nm; and complexes **6a** (two fluorene units) to **6c** (four fluorene units) from 572–586 nm by increasing the number of fluorene units. The emission spectra of **1**, **2**, **3a–g**, **4a–d**, **5a–c** and **6a–c** in glassy solutions (DMF:MeOH:EtOH mixture, v:v:v=1:1:4) at 77 K and

their solid-state emission spectra are given in the Supporting Information (Figures S41–S59). In general, the complexes display vibronic-structured emission bands with emission energies similar to those observed in dichloromethane. For example, the emission of **3a** exhibits peak maxima λ_{max} at 553, 575, 600 and 650 nm (vibronic progression $\approx 1300 \text{ cm}^{-1}$) in DMF:MeOH:EtOH glassy solution (v:v:v=1:1:4) at 77 K. The solid-state emission maxima of complexes **1**, **2**, **3a–g**, **4a–d**, **5a–c** and **6a–c** at room temperature are in the range from 560 to 650 nm. The vibronic structures are better resolved after cooling the solid samples to 77 K. These emission bands are similarly assigned to mixed $^3\text{IL}/^3\text{MLCT}$ states.

OLED fabrication and electroluminescent properties: The fluorene-based cyclometalated platinum(II) complexes display high emission quantum yields and high thermal stability, both of which are required features of advanced materials for OLED applications. The OLEDs studied in this work were prepared by vacuum deposition and spin-coat methods. Monochromic OLEDs were fabricated with 2–8 wt% of platinum(II) complexes as the emitting dopant and with the following configurations: ITO (indium tin oxide)/NPB (4,4'-bis[*N*-(1-naphthyl)*N*-phenylamino]biphenyl, 40 nm)/CBP (4,4'-*N,N'*-dicarbazolebiphenyl): Pt^{II} complex (2–8 wt%, 30 nm)/BCP (2,9-dimethyl-4,7-diphenyl-1,10-phenanthroline, 15 nm)/Alq₃ (tris(8-quinolinolato)aluminium, 30 nm)/LiF (0.5 nm)/Al (100 nm). The spin-coat device adopted a similar configuration: ITO/PEDOT:PSS/PVK: Pt^{II} complex (5 wt%, 80 nm)/BCP (15 nm)/Alq₃ (30 nm)/LiF (0.5 nm)/Al (100 nm). Schematic cross-section diagrams of the device structure are depicted in the Supporting Information (Figures S60 and S61), and a summary of the device performances is given in Table 3.

Devices **A–G** gave yellow or orange light with similar CIE coordinates. These OLED devices displayed a strong emission with peak maxima at 560–585 nm and a shoulder at about 610–630 nm (Figure 5). Both the band shape and emission maximum of the electroluminescence (EL) are similar to that of the corresponding photoluminescence (PL). The EL is tentatively assigned to the same mixed $^3\text{IL}/^3\text{MLCT}$ excited state as that for the corresponding PL of the platinum(II) complex. The EL spectra of devices **A–G** remained unchanged at a high operation voltage of 15–20 V. In all cases, there was no undesirable emission from the host material or Alq₃ layer, revealing efficient energy transfer from the CBP or PVK host material to the dopant complexes.

The turn-on voltages for the vacuum-deposited devices were in the range of 5 to 6 V. The maximum brightness of 29000 cd m^{-2} was achieved at 17 V for device **D**. The operation voltages for devices **A–D** are similar to the reported values found for related [PtCl(R-C^{^N}^N)]^[11a] and [PtCl(O^{^N}^N)]^[15]-based OLEDs. Device **B** was found to display a similar maximum brightness (27000 cd m^{-2}), with a maximum current efficiency and power efficiency of 14.7 cd A^{-1} and 9.2 Lm W^{-1} , respectively (Table 3, Figure 6). The current

Table 3. Electroluminescence data for **3a**, **3d**, **3f**, **3g**, **5d**, **5c** and **6c**.

Device (Complex)	$x^{[a]}$ [%]	$B_{\max}^{[b]}$ [cd m^{-2}]	$\text{CIE}^{[c]}$ / x, y	$\eta_{\text{cmax}}^{[d]}$ [cd A^{-1}]	$\eta_{\text{pmax}}^{[e]}$ [lm W^{-1}]	$\text{EQE}_{\max}^{[f]}$ [%]	Fabrication method
A (3a)	4	27000	0.53, 0.45	10.6	5.3	3.3	vacuum deposition
B (3d)	2	27000	0.53, 0.46	14.7	9.2	5.5	vacuum deposition
C (5b)	3.5	8300	0.52, 0.43	3.8	1.7	1.3	vacuum deposition
D (5c)	8	29000	0.44, 0.54	13.9	5.5	4.2	vacuum deposition
E (3f)	5	3500	0.52, 0.47	9.2	3.7	3.4	spin-coating
F (3g)	5	1000	0.56, 0.42	3.2	1.3	1.5	spin-coating
G (6c)	5	1900	0.55, 0.43	2.5	0.8	1.0	spin-coating

[a] Dopant concentration of Pt^{II} complex. [b] Maximum brightness. [c] Commission Internationale de L'Eclairage coordinates. [d] Maximum current efficiency. [e] Maximum power efficiency. [f] Maximum external quantum efficiency.

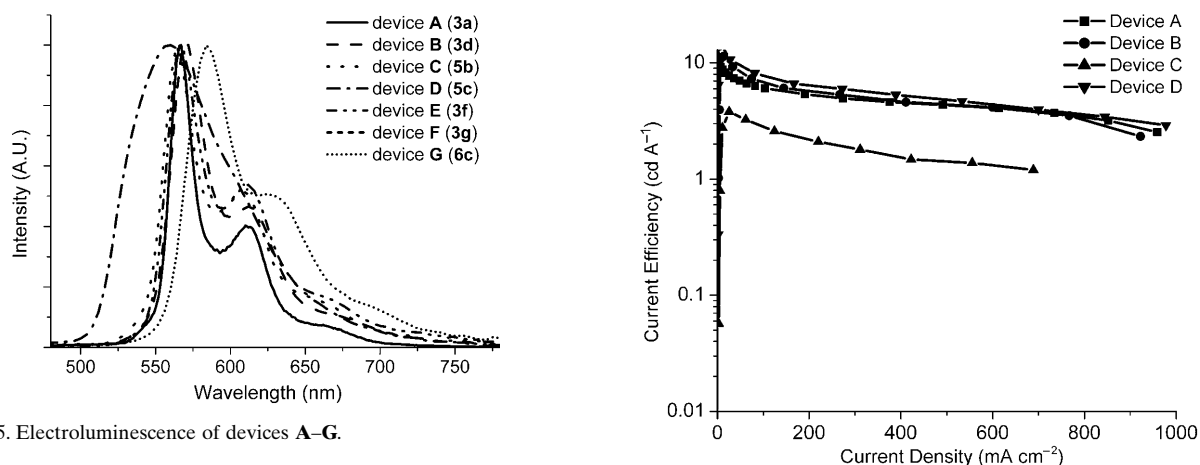


Figure 5. Electroluminescence of devices **A–G**.

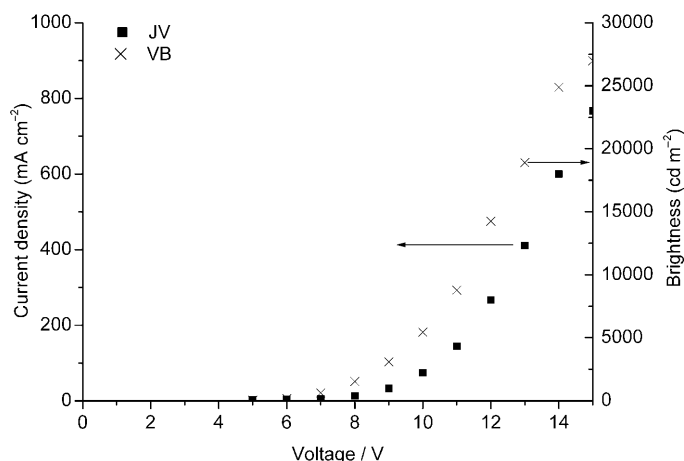


Figure 6. Current–voltage–brightness (J–V–B) relationship of device **B** (Complex **3d**).

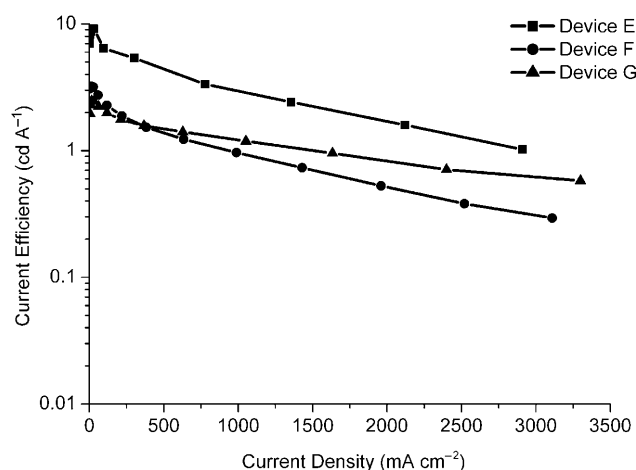


Figure 7. Current efficiency for vacuum-deposited OLED devices **A–D** (top) and spin-coated OLED devices **E–G** (bottom).

efficiency and current density relationships for devices **A–G** are depicted in Figure 7. The brightness and device efficiency are comparable to those devices fabricated with $[\text{PtCl}(\text{R}^{\wedge}\text{N}^{\wedge}\text{N})]^{[11a]}$ and $[\text{PtCl}(\text{O}^{\wedge}\text{N}^{\wedge}\text{N})]^{[15]}$ complexes as phosphorescent dopants.

Solution-processed OLEDs were fabricated using poly(9-vinylcarbazole) (PVK) as host material. The increased solubility imparted by the two *n*-hexyl chains on each fluorene unit could facilitate homogeneous film formation with the polymer host (Figure S72). It is known that the crystallisation process leads to the formation of traps for charge carriers, which decreases the OLED device performance. The

turn-on voltage of the spin-coated devices **E–G** are in the range of 6 to 7 V, similar to that of PVK-hosted Ir^{III} complex devices.^[17] The relatively higher driving voltage compared to the vacuum-deposited devices could be attributed to the thicker light-emitting layer in the spin-coated devices (PVK:Pt, 80 nm; CBP:Pt, 30 nm). A maximum brightness of 3500 cd m^{-2} was achieved for device **E** with a good current efficiency (9.2 cd A^{-1}). Although a number of highly efficient OLED devices have been fabricated using cyclometalated platinum(II) complexes as phosphorescent dopants using the vacuum deposition technique,^[10,11,15] the results de-

scribed in this work represent the first study of platinum(II) complexes as suitable phosphorescent dopants in both vacuum-deposited organic light-emitting diodes as well as solution-processed devices with polymeric host materials. Further studies on the use of different host materials, device thicknesses, and the use of additional electron transport material(s) would provide information for improving the performance of the solution-processed OLEDs using platinum(II) complexes as dopants.

Conclusion

In summary, a series of new C[^]N[^]N cyclometalated ligands containing fluorene units and their corresponding platinum(II) complexes have been synthesised and characterised. The crystal structures of the platinum(II) complexes reveal extensive intermolecular π - π interactions among the fluorene-containing C[^]N[^]N ligands. The electronic absorption and emission spectra of the platinum(II) complexes have been studied. Vibronic-structured emission bands have been observed, which are tentatively assigned to triplet excited states having mixed intraligand (³IL) π - π^* and metal-to-ligand charge transfer (³MLCT) character. When the number of fluorene units increases from one to two (**3a-g**; **5a-c**) and from two to four (**6a-c**), a small red shift in emission energy is observed. These highly emissive platinum(II) complexes display good thermal stability, rendering them suitable materials for OLED applications. Their high solubility in common organic solvents such as toluene enable the complexes to be doped into a polymer host by various solution-processing techniques, such as ink-jet printing or the spin-coating method. These complexes are yellow to orange dopants for OLEDs with good device efficiencies. The performances of the vacuum-deposited or solution-processed OLED are comparable to those of the related Pt^{II}_[10,11,15] or Ir^{III}-based devices.^[7,17]

Experimental Section

Instrumentation: Electron-impact (EI) and fast atom bombardment (FAB) mass spectra were obtained on a Finnigan Mat 95 mass spectrometer. ¹H and ¹³C NMR spectra were recorded on Bruker AVANCE 600, DRX 400 and 300 FT-NMR spectrometers. ¹H and ¹³C NMR chemical shifts were referenced to TMS (TMS=tetramethylsilane) and residual proton/carbon atoms of CDCl₃, CD₂Cl₂ and d₇-DMF. Peak assignments were based on ¹H-¹H correlation and NOESY 2D NMR experiments. Elemental analyses were performed at the Institute of Chemistry at the Chinese Academy of Science, Beijing. UV/Vis spectra were obtained with a Hewlett-Packard 8452 A spectrophotometer. Excitation and emission spectra were recorded on Spex Fluorolog-3 model fluorescence spectrofluorometer. All solutions for photophysical studies were degassed on a vacuum line with no fewer than three successive freeze-pump-thaw cycles. Excited-state lifetimes were measured using a Nd:YAG laser. Luminescence quantum yields were measured using [Ru(bpy)₃]₂Cl₂ in degassed acetonitrile as reference. Cyclic voltammetric measurements were performed using a Princeton Applied Research electrochemical analyser with a conventional three-compartment cell. Electrochemical measurements were performed in DMF with 0.1 M nBu₄NPF₆ (TBAH) as support-

ing electrolyte at room temperature. All solutions for electrochemical studies were deaerated with pre-purified argon gas before measurements. The reference electrode was Ag/AgNO₃ (0.1 M in acetonitrile), the working electrode was a glassy carbon electrode and a platinum wire was used as the counter electrode. Ferrocene was used as the internal reference.

Synthesis of fluorene-based C[^]N[^]N ligands and corresponding platinum(II) complexes: The fluorene-based C[^]N[^]N ligands were prepared by in situ generation of the pyridine ring through the cyclisation of ketone with ammonium salt,^[11a] followed by a Suzuki coupling reaction. The synthetic scheme and procedures, and the characterisations of the starting materials (S1-S29) and ligands are described in the Supporting Information. The platinum(II) complexes were prepared by heating under reflux a mixture of K₂PtCl₄ and the corresponding fluorene-based C[^]N[^]N ligands in a chloroform/glacial acetic acid mixture (v:v 1:9, 50 mL) for 24 h. The orange solid was filtered, washed with water and diethyl ether and recrystallised in CH₂Cl₂ to give an orange crystalline solid. Both ligands and corresponding platinum(II) complexes were characterised by ¹H NMR spectroscopy, FAB or ESI mass spectrometry and elemental analyses. ¹H NMR spectra were assigned with ¹H-¹H COSY and NOESY experiments.

Complex 1: Yield: 86%; ¹H NMR (400 MHz, CDCl₃): δ = 0.77–0.86 (m, 10H; -CH₂- and -CH₃), 1.12–1.18 (m, 12H; -CH₂-), 1.97–2.02 (m, 4H; -CH₂-), 7.17 (s, 1H; H¹³), 7.22–7.34 (m, 5H; H⁷, H⁸, H⁹, H¹⁵ and H²¹), 7.47–7.51 (m, 2H; H²⁶ and H²⁷), 7.52 (d, J = 7.5 Hz, 1H; H⁶), 7.62–7.73 (m, 2H; H¹⁷ and H²⁵), 7.81 (s, 1H; H³), 7.89 (t, J = 7.5 Hz, 1H; H²²), 7.98 (d, J = 7.2 Hz, 1H; H²³), 8.71 ppm (s, 1H; H²⁰); FAB-MS (+ve): m/z : 793 [M^+]; elemental analysis calcd (%) for C₄₁H₄₃N₂PtCl: C 61.99, H 5.46, N 3.53; found: C 61.84, H 5.64, N 3.54.

Complex 2: Yield: 86%; ¹H NMR (400 MHz, CDCl₃): δ = 0.66–0.89 (m, 10H; -CH₂- and -CH₃), 1.11–1.31 (m, 12H; -CH₂-), 2.06–2.16 (m, 4H; -CH₂-), 2.09–2.20 (m, 2H; -CH₂-), 6.91 (t, J = 7.0 Hz, 1H, H⁵), 7.15–7.19 (m, 3H; H⁶, H⁸ and H¹⁴), 7.33 (d, J = 7.3 Hz, 1H, H³), 7.39–7.43 (m, 2H; H⁴ and H²²), 7.78–7.81 (m, 4H; H⁶, H¹⁰, H²⁵ and H²⁹), 7.82 (d, J = 7.4 Hz, 1H, H¹⁹), 7.90–8.10 (m, 2H; H¹⁵ and H¹⁶), 8.95 ppm (d, J = 4.8 Hz, 1H, H²³); FAB-MS (+ve): m/z : 793 [M^+]; elemental analysis calcd (%) for C₄₁H₄₃N₂PtCl: C 61.99, H 5.46, N 3.53; found: C 61.95, H 5.50, N 3.51.

Complex 3a: Yield: 90%; ¹H NMR (500 MHz, CD₂Cl₂): δ = 0.66–0.81 (m, 4H; CH₂), 0.77 (t, J = 7.1 Hz, 6H; -CH₃), 1.04–1.17 (m, 12H; -CH₂-), 1.98–2.08 (m, 12H; -CH₂-), 7.32 (s, 1H; H¹³), 7.32–7.39 (m, 4H; H⁷, H⁸, H⁹ and H¹⁵), 7.63 (d, J = 7.4 Hz, 1H; H¹⁷), 7.69 (t, J = 7.8 Hz, 1H; H²³), 7.72 (t, J = 7.9 Hz, 1H; H¹⁶), 7.81 (d, J = 7.5 Hz, 1H; H⁶), 7.85 (t, J = 8.1 Hz, 1H; H²⁴), 7.93 (d, J = 8.2 Hz, 1H; H²²), 7.96 (d, J = 8.1 Hz, 1H; H²⁵), 7.98 (s, ³JH-Pt = 21.1 Hz, 1H; H³), 8.33 (s, 1H; H²⁷), 9.46 ppm (s, 1H; H²⁰); FAB-MS: m/z : 767 [M^+]; elemental analysis calcd (%) for C₃₉H₄₁N₂PtCl: C 60.97, H 5.38, N 3.65; found: C 61.94, H 5.34, N 3.62.

Complex 3b: Yield: 90%; ¹H NMR (500 MHz, CD₂Cl₂): δ = 0.74–0.89 (m, 10H; -CH₂- and -CH₃), 1.12–1.23 (m, 12H; -CH₂-), 2.00–2.06 (m, 4H; -CH₂-), 7.21 (t, J = 7.8 Hz, 1H; H¹³), 7.30–7.51 (m, 6H; H³⁰, H³¹ and H³³), 7.60–7.75 (m, 4H; H³² and H³⁵), 7.76–7.80 (m, 2H; H¹⁵ and H¹⁷), 7.81 (d, J = 7.1 Hz, 1H; H³), 7.87 (t, J = 7.9 Hz, 1H; H¹⁶), 7.99 (d, J = 7.2 Hz, 1H; H⁶), 8.00 (d, J = 8.3 Hz, 2H; H³ and H²⁴), 8.24 (d, J = 8.2 Hz, 1H; H²⁵), 8.35 (s, 1H; H²²), 8.52 (s, 1H; H²⁷), 9.52 ppm (s, 1H; H²⁰); FAB-MS (+ve): m/z : 944 [M^+]; elemental analysis calcd (%) for C₅₃H₄₉N₂PtCl: C 67.40, H 5.23, N 2.97; found: C 67.39, H 5.21, N 3.01.

Complex 3c: Yield: 90%; ¹H NMR (500 MHz, CD₂Cl₂): δ = 0.71–0.83 (m, 10H; -CH₂- and -CH₃), 1.11–1.24 (m, 12H; -CH₂-), 1.99–2.03 (m, 4H; -CH₂-), 6.88–6.98 (m, 2H; H⁷ and H⁺), 7.02 (d, J = 7.3 Hz, 1H; H²⁹), 7.15 (s, 1H; H⁹), 7.30–7.47 (m, 2H; H³⁵ and H⁴¹), 7.49 (t, J = 7.9 Hz, 1H; H³⁶), 7.51 (t, J = 8.1 Hz, 1H; H⁴⁰), 7.52–7.63 (m, 4H; H⁶, H¹⁶, H¹⁷ and H²⁴), 7.72–7.84 (m, 4H; H³, H²³, H²⁵ and H³⁹), 7.91 (t, J = 7.0 Hz, 2H; H²² and H³⁷), 8.01 (d, J = 7.9 Hz, 1H; H³⁴), 8.32 (s, 1H; H²⁷), 9.36 ppm (s, 1H; H²⁰); FAB-MS (+ve): m/z : 984 [M^+]; elemental analysis calcd (%) for C₅₅H₅₂N₃PtCl: C 67.03, H 5.32, N 4.26; found: C 66.93, H 5.27, N 4.38.

Complex 3d: Yield: 85%; ¹H NMR (400 MHz, CD₂Cl₂): δ = 0.65–0.86 (m, 10H; -CH₂- and -CH₃), 1.12–1.24 (m, 12H; -CH₂-), 2.02–2.09 (m, 4H; -CH₂-), 7.13 (s, 1H; H¹³), 7.18 (s, 1H; H¹³), 7.30–7.34 (m, 3H; H³⁰ and H³¹), 7.44–7.49 (m, 6H; H⁷, H⁸, H²⁴, H²⁵ and H²⁹), 7.63 (s, 1H; H³), 7.73–7.81 (m, 3H; H⁶, H⁹ and H²³), 7.90 (s, 1H; H¹⁷), 7.90 (d, J = 8.2 Hz, 1H;

H²²), 8.36 (s, 1H; H²⁷), 9.09 ppm (s, 1H; H²⁰); FAB-MS: *m/z*: 844 [*M*⁺]; elemental analysis calcd (%) for C₄₅H₄₅N₂PtCl: C 64.01, H 5.37, N 3.32; found: C 64.08, H 5.31, N 3.26.

Complex 3e: Yield: 79%; ¹H NMR (400 MHz, CD₂Cl₂): δ = 0.62–0.78 (m, 10H; -CH₂- and -CH₃), 1.08–1.15 (m, 12H; -CH₂-), 2.00–2.11 (m, 4H; -CH₂-), 7.43–7.47 (m, 5H; H¹³, H¹⁵, H³⁰ and H³¹), 7.49–7.56 (m, 5H; H⁷, H²⁴, H²⁵, H²⁹), 7.65 (m, 1H; H³), 7.81–7.85 (m, 3H; H⁶, H⁹ and H²³), 7.88 (s, 1H; H¹⁷), 8.02 (d, *J* = 7.6 Hz, 1H; H²²), 8.47 (s, 1H; H²⁷), 9.43 ppm (s, 1H; H²⁰); FAB-MS (+ve): *m/z*: 984 [*M*⁺]; elemental analysis calcd (%) for C₅₅H₅₂N₃PtCl: C 75.86, H 6.08, N 4.83; found: C 75.81, H 6.03, N 4.91.

Complex 3f: Yield: 85%; ¹H NMR (400 MHz, CD₂Cl₂): δ = 0.65–0.86 (m, 10H; -CH₂- and -CH₃), 1.12–1.24 (m, 12H; -CH₂-), 2.02–2.09 (m, 4H; -CH₂-), 7.20 (s, 1H; H¹³), 7.24–2.29 (m, 4H; H⁷, H⁸, H⁹ and H¹⁵), 7.47 (t, *J* = 7.2 Hz, 1H; H²⁴), 7.58 (s, 1H; H³¹), 7.62 (s, 3H; H⁶ and H²⁹), 7.68–7.72 (m, 3H; H¹⁷, H²³ and H²⁵), 7.90 (d, *J* = 8.1 Hz, 1H; H²²), 7.94 (s, 1H; H³), 8.33 (s, 1H; H²⁷), 9.48 ppm (s, 1H; H²⁰); FAB-MS (+ve): *m/z*: 955 [*M*⁺]; elemental analysis calcd (%) for C₅₃H₆₁N₂PtCl: C 64.01, H 5.37, N 3.32; found: C 64.08, H 5.33, N 3.29.

Complex 3g: Yield: 80%; ¹H NMR (400 MHz, CD₂Cl₂): δ = 0.70–0.97 (m, 20H; -CH₂- and -CH₃), 1.08–1.29 (m, 24H; -CH₂-), 2.02–2.25 (m, 8H; -CH₂-), 7.19 (s, 1H; H¹⁵), 7.23 (s, 1H; H¹³), 7.31–7.39 (m, 3H; H³⁸, H³⁹ and H⁴⁰), 7.47–7.55 (m, 5H; H²⁴, H²⁵, H³⁰ and H³¹), 7.59 (d, *J* = 8.0 Hz, 1H; H³³), 7.65–7.68 (m, 3H; H³, H³⁴ and H⁴⁴), 7.72 (s, 1H; H¹⁷), 7.73 (d, *J* = 8.0 Hz, 1H; H³⁷), 7.76–7.85 (m, 6H; H⁶, H⁷, H⁹, H²³ and H²⁹), 7.92 (d, *J* = 8.3 Hz, 1H; H²²), 8.37 (s, 1H; H²⁷), 9.15 ppm (s, 1H; H²⁰); FAB-MS: *m/z*: 1177 [*M*⁺]; elemental analysis calcd (%) for C₇₀H₇₇N₂PtCl: C 71.44, H 6.59, N 2.38; found: C 71.31, H 6.60, N 2.42.

Complex 4a: Obtained as a 1:1 mixture of structural isomers A and B. Yield: 75%; ¹H NMR (400 MHz, CD₂Cl₂): δ = 0.72–0.95 (m, 20H; -CH₂- and -CH₃), 1.12–1.30 (m, 24H; -CH₂-), 1.99–2.24 (m, 8H; -CH₂-), 7.37–7.49 (m, 10H; Ar-H), 7.61 (m, 2H; Ar-H), 7.68–7.83 (m, 6H; Ar-H), 7.85–7.86 (m, 18H; Ar-H), 8.11–8.23 (m, 2H; Ar-H), 8.43 (s, 1H; H₂₄), 8.51 (s, 1H; H₂₄), 9.71 (d, *J* = 7.3 Hz, 1H; H⁸), 9.79 (s, 1H; H¹⁷), 10.02 ppm (s, 1H; H¹⁷); FAB-MS (+ve): *m/z*: 893 [*M*⁺].

Complex 4b: Obtained as a 1:0.5 mixture of isomers A and B. Yield: 77%; ¹H NMR (400 MHz, *d*₇-DMF): δ = 0.75–0.93 (m, 12H; -CH₂- and -CH₃), 1.14–1.28 (m, 15H; -CH₂-), 2.53–2.60 (m, 6H; -CH₂-), 7.52–7.69 (m, 3H; Ar-H), 7.72 (d, *J* = 7.6 Hz, 1.5H; Ar-H), 7.89 (d, *J* = 7.3 Hz, 1H; Ar-H), 7.91–7.97 (m, 2.5H; Ar-H), 8.02 (s, 1H; Ar-H), 8.32–8.47 (m, 7H; Ar-H), 8.48 (s, 1H; Ar-H), 8.49–8.52 (m, 4H; Ar-H), 8.67–8.73 (m, 4H; Ar-H), 8.92 (s, 1.5H; Ar-H), 9.12 (s, 1H; Ar-H), 8.52 (s, 1H; H²⁴), 8.52 (s, 0.5H; H²⁴), 10.02 (s, 1H; H¹⁷), 10.08 (d, *J* = 7.2 Hz, 0.5H; H⁸), 10.25 ppm (s, 1H; H¹⁷); FAB-MS (+ve): *m/z*: 971 [*M*⁺].

Complex 4c: Obtained as a 1:1 mixture of isomers A and B. Yield: 72%; ¹H NMR (400 MHz, CD₂Cl₂): δ = 0.65–0.92 (m, 42H; -CH₂- and -CH₃), 1.15–1.32 (m, 44H; -CH₂-), 2.01–2.18 (m, 8H; -CH₂-), 2.27–2.43 (m, 8H; -CH₂-), 7.11 (d, *J* = 7.3 Hz, 1H; Ar-H), 7.22–7.34 (m, 2H; Ar-H), 7.38–7.49 (m, 16H; Ar-H), 7.58–7.70 (m, 8H; Ar-H), 7.74–7.82 (m, 6H; Ar-H), 7.83–7.91 (m, 4H; Ar-H), 7.96–8.01 (m, 6H; Ar-H), 8.06 (s, 1H; H²⁴), 8.12 (s, 1H; H²⁴), 9.29 (s, 1H; H¹⁷), 9.46 (d, *J* = 7.4 Hz, 1H; H⁸), 9.58 ppm (s, 1H; H¹⁷); FAB-MS (+ve): *m/z*: 1225 [*M*⁺].

Complex 4d: Obtained as a 1:1 mixture of isomers A and B. Yield: 82%; ¹H NMR (400 MHz, CD₂Cl₂): δ = 0.68–0.82 (m, 9H; -CH₂-), 0.82–0.91 (m, 11H; -CH₂- and -CH₃), 1.13–1.28 (m, 24H; -CH₂-), 2.12–2.27 (m, 8H; -CH₂-), 6.97 (d, *J* = 7.1 Hz, 1H; Ar-H), 7.02 (s, 1H; Ar-H), 7.17–7.38 (m, 14H; Ar-H), 7.52–7.68 (m, 18H; Ar-H), 7.78 (d, *J* = 7.3 Hz, 1H; Ar-H), 7.83 (d, *J* = 7.4 Hz, 1H; Ar-H), 7.92 (s, 1H; H²⁴), 8.02 (s, 1H; H²⁴), 8.89 (s, 1H; H¹⁷), 9.18 (s, 1H; H¹⁷), 9.43 ppm (d, *J* = 7.3 Hz, 1H; H⁸); FAB-MS (+ve): *m/z*: 971 [*M*⁺].

Complex 5a: Yield: 86%; ¹H NMR (400 MHz, CD₂Cl₂): δ = 0.69–0.89 (m, 10H; -CH₂- and -CH₃), 1.08–1.39 (m, 12H; -CH₂-), 2.08–2.16 (m, 4H; -CH₂-), 7.13 (t, *J* = 7.5 Hz, 1H; H²⁸), 7.18 (t, *J* = 6.4 Hz, 1H; H²⁷), 7.39–7.45 (m, 3H; H³, H⁴ and H⁵), 7.50 (d, *J* = 7.5 Hz, 1H; H²⁹), 7.69 (t, *J* = 6.4 Hz, 1H; H¹⁷), 7.785–7.85 (m, 3H; H⁶, H²² and H³³), 7.92–7.96 (m, 2H; H¹⁶ and H²³), 7.98 (s, 1H; H¹⁰), 8.04 (d, *J* = 8.2 Hz, 1H; H¹⁵), 8.11 (d, *J* = 8.0 Hz, 1H; H¹⁸), 8.51 (s, 1H; H²⁰), 9.70 ppm (s, 1H; H¹³); FAB-MS (+ve):

m/z: 844 [*M*⁺]; elemental analysis calcd (%) for C₄₅H₄₅N₂PtCl: C 64.01, H 5.37, N 3.32; found: C 63.98, H 5.33, N 3.27.

Complex 5b: Yield: 86%; ¹H NMR (400 MHz, CD₂Cl₂): δ = 0.72–0.81 (m, 10H; -CH₂- and -CH₃), 1.11–1.22 (m, 12H; -CH₂-), 2.02–2.09 (m, 4H; -CH₂-), 2.02–2.13 (m, 2H; -CH₂-), 2.19–2.25 (m, 2H; -CH₂-), 6.94 (t, *J* = 7.2 Hz, 1H; H⁴), 6.99 (t, *J* = 7.2 Hz, 1H; H³), 7.23 (d, *J* = 7.0 Hz, 1H; H⁶), 7.30 (s, 1H; H⁸), 7.47 (d, *J* = 7.4 Hz, 1H; H³), 7.55–7.63 (m, 3H; H²², H²⁷ and H²⁹), 7.72–7.76 (m, 2H; H¹⁸ and H²⁶), 7.82 (t, *J* = 7.5 Hz, 1H; H¹⁷), 7.86–7.93 (m, 5H; H¹⁰, H¹⁵, H¹⁶, H²³ and H³³), 8.39 (s, 1H; H²⁰), 9.33 ppm (s, 1H; H¹³); FAB-MS (+ve): *m/z*: 923 [*M*⁺]; elemental analysis calcd (%) for C₄₅H₄₄N₂BrPtCl: C 58.54, H 4.80, N 3.03; found: C 58.57, H 4.81, N 3.05.

Complex 5c: Yield: 86%; ¹H NMR (400 MHz, CD₂Cl₂): δ = 0.76–0.87 (m, 10H; -CH₂- and -CH₃), 1.01–1.38 (m, 12H; -CH₂-), 2.06–2.15 (m, 2H; -CH₂-), 2.23–2.33 (m, 2H; -CH₂-), 7.08 (m, 2H; H⁴⁰ and H⁴¹), 7.37 (t, *J* = 7.5 Hz, 1H; H⁵), 7.42 (m, 1H; H²), 7.49 (t, *J* = 7.3 Hz, 1H; H⁴²), 7.57 (s, 1H; H⁶), 7.60–7.63 (m, 2H; H³⁵ and H³⁹), 7.64–7.77 (m, 6H; H⁴, H²², H²⁷, H²⁹, H³⁶ and H⁴⁶), 7.83–8.02 (m, 8H; H¹⁰, H¹⁵, H¹⁶, H¹⁷, H¹⁸, H²³, H²⁶ and H³³), 8.48 (s, 1H; H²⁰), 9.56 ppm (s, 1H; H¹³); FAB-MS (+ve): *m/z*: 1175 [*M*⁺]; elemental analysis calcd (%) for C₇₀H₇₇N₂PtCl: C 58.54, H 4.80, N 3.03; found: C 58.58, H 4.83, N 2.99.

Complex 6a: Yield: 80%; ¹H NMR (400 MHz, CD₂Cl₂): δ = 0.70–0.97 (m, 20H; -CH₂- and -CH₃), 1.08–1.29 (m, 24H; -CH₂-), 2.02–2.25 (m, 8H; -CH₂-), 7.33–7.38 (m, 3H; H³⁴, H³⁵ and H³⁶), 7.40–7.52 (m, 3H; H⁷, H⁸ and H⁹), 7.52 (s, 1H; H³), 7.79–7.97 (m, 9H; H⁶, H¹³, H¹⁵, H²³, H²⁴, H²⁹, H³⁰, H³³ and H⁴⁰), 8.05 (d, *J* = 8.2 Hz, 1H; H²⁵), 8.10 (s, 1H; H¹⁷), 8.18 (d, *J* = 8.1 Hz, 1H; H²⁵), 8.55 (s, 1H; H²⁷), 9.81 ppm (s, 1H; H²⁰); FAB-MS (+ve): *m/z*: 1100 [*M*⁺]; elemental analysis calcd (%) for C₆₄H₇₃N₂PtCl: C 69.83, H 6.68, N 2.54; found: C 69.71, H 6.70, N 2.56.

Complex 6b: Yield: 80%; ¹H NMR (400 MHz, CD₂Cl₂): δ = 0.70–0.97 (m, 20H; -CH₂- and -CH₃), 1.08–1.29 (m, 24H; -CH₂-), 2.02–2.25 (m, 8H; -CH₂-), 7.33–7.38 (m, 3H; H³⁴, H³⁵ and H³⁶), 7.40–7.52 (m, 3H; H⁷, H⁸ and H⁹), 7.52 (s, 1H; H³), 7.79–7.97 (m, 9H; H⁶, H¹³, H¹⁵, H²³, H²⁴, H²⁹, H³⁰, H³³ and H⁴⁰), 8.05 (d, *J* = 8.2 Hz, 1H; H²⁵), 8.10 (s, 1H; H¹⁷), 8.18 (d, *J* = 8.1 Hz, 1H; H²⁵), 8.55 (s, 1H; H²⁷), 9.81 ppm (s, 1H; H²⁰); FAB-MS (+ve): *m/z*: 1256 [*M*⁺]; elemental analysis calcd (%) for C₆₄H₇₁N₂Br₂PtCl: C 61.07, H 5.69, N 2.23; found: C 60.95, H 5.63, N 2.23.

Complex 6c: Yield: 80%; ¹H NMR (400 MHz, CD₂Cl₂): δ = 0.63–0.92 (m, 20H; -CH₂- and -CH₃), 1.06–1.33 (m, 24H; -CH₂-), 2.04–2.25 (m, 8H; -CH₂-), 7.31–7.41 (m, 6H; H⁴⁷, H⁴⁸, H⁴⁹, H⁶⁰, H⁶¹ and H⁶²), 8.08 (d, *J* = 8.4 Hz, 1H; H²²), 8.14 (s, 1H; H¹⁷), 8.18 (d, *J* = 8.0 Hz, 1H; H²⁵), 8.58 (s, 1H; H²⁷), 9.82 ppm (s, 1H; H²⁰); FAB-MS (+ve): *m/z*: 1765 [*M*⁺]; elemental analysis calcd (%) for C₁₁₄H₁₃₇N₂PtCl: C 77.54, H 7.82, N 1.59; found: C 77.60, H 7.85, N 1.54.

Single-crystal structure determination: X-ray diffraction data of complexes **2**, **3c** and **4c** were collected on a Bruker X8 Proteum diffractometer using Cu_{Kα} radiation (1.54178 Å), and the X-ray diffraction data of **3a** were collected on a Bruker Smart CCD 1000 using graphite monochromatised Mo_{Kα} radiation (0.71073 Å). The images were interpreted and intensities were integrated using the PROTEUM2 suite or DENZO program. The structure was solved by the direct method employing the SHELXS-97 program. Full-matrix least-squares refinements on *F*² were used in the structure refinement. The positions of H atoms were calculated on the basis of the riding mode with thermal parameters equal to 1.2 times those of the associated C atoms, and participated in the calculation of final *R* indices. In the final stage of the least-square refinements, all non-hydrogen atoms were refined anisotropically.

OLED fabrication: The vapour-deposited- and spin-coated OLED devices fabricated utilised a multilayer sandwich device structure. Indium tin oxide (ITO) was used as anode and ITO glass was cleaned according to the following procedure before OLED fabrication. ITO glass was sonicated in detergent solution for 10 min at 60 °C for degreasing, then sonicated in deionised water to remove the detergent. It was subsequently sonicated in ethanol, toluene and acetone for 10 min at 60 °C, dried with a nitrogen blowgun, and heated at 120 °C for 1 h. The ITO glass was treated in a UV ozone cleaner for 25 min before loading onto the vacuum deposition chamber. All materials were deposited onto the ITO glass by thermal deposition at a pressure of 1 × 10⁻⁶ Torr. The vacuum-deposited

devices were fabricated by the following procedures: *N,N'*-bis(1-naphthyl)-1,1'-biphenyl-4,4'-diamine (NPB, 30 nm) was first deposited onto the ITO glass as hole transport layer, followed by a light-emitting layer with 4,4'-*N,N'*-dicarbazolebiphenyl (CBP, 30 nm) as host and 2–8 wt % of platinum complex as phosphorescent dopant. The dopant level was controlled by the deposition rates. The 2,9-dimethyl-4,7-diphenyl-1,10-phenanthroline exciton confining layer (BCP, 15 nm) and electron transport and injection layers (Alq₃, 30 nm), LiF (0.5 nm) and Al (100 nm) were subsequently deposited. The spin-coated devices were fabricated by the following procedures: a layer of poly(3,4-ethylenedioxythiophene)/poly(styrenesulfonate) (PEDOT/PSS) was spin-coated onto the substrate at 8000 rpm and baked at 90 °C for 45 min. Fluorene-based platinum(II) complexes (2–8 wt %) and the PVK polymer host were dissolved in chlorobenzene. The resulting solutions were filtered through 0.45 μm filters prior to use. The solutions were spin-cast at 2000 rpm for 30 s and baked at 90 °C for 1 h. The film thicknesses were determined to be in the approximate range of 1000–1200 Å by ellipsometry. The BCP, Alq₃, LiF and Al layers were subsequently deposited under the same vacuum deposition conditions as the vacuum-deposited OLEDs.

Acknowledgements

We gratefully acknowledge financial support from the Innovation and Technology Commission of the HKSAR Government (ITF/016/08NP), the University Grants Committee of the Hong Kong SAR (AoE/P-03/08), the Research Grants Council of Hong Kong SAR (HKU 7008/09P), the National Natural Science Foundation of China/Research Grants Council Joint Research Scheme (N HKU 752/08) and the Chinese Academy of Sciences: Croucher Foundation Funding Scheme For Joint Laboratories. Dr. S. C. F. Kui acknowledges the small project funding (200807176030) and the postdoctoral fellow scholarship from The University of Hong Kong. Dr. M.-Y. Yuen acknowledges the postgraduate studentship from The University of Hong Kong.

- [1] First OLED: C. W. Tang, S. A. VanSlyke, *Appl. Phys. Lett.* **1987**, *51*, 913–915.
- [2] a) T. Watanabe, H. S. Nalwa, S. Miyata in *Organic Electroluminescent Materials and Devices* (Ed.: S. Miyata, H. S. Nalwa), Gordon and Breach, Amsterdam, **1997**, pp. 459–482; b) F. Hide, M. A. Díaz-García, B. J. Schwartz, A. J. Heeger, *Acc. Chem. Res.* **1997**, *30*, 430–436; c) R. H. Friend, *Pure Appl. Chem.* **2001**, *73*, 425–430; d) W. Lu, B.-X. Mi, M. C. W. Chan, Z. Hui, N. Zhu, S.-T. Lee, C.-M. Che, *Chem. Commun.* **2002**, 206–207; e) C.-M. Che, S.-C. Chan, H.-F. Xiang, M. C. W. Chan, Y. Liu, Y. Wang, *Chem. Commun.* **2004**, 1484–1485; f) S.-W. Lai, C.-M. Che, *Top. Curr. Chem.* **2004**, *241*, 27–63; g) H.-F. Xiang, S.-W. Lai, P. T. Lai, C.-M. Che in *Highly Efficient OLEDs with Phosphorescent Materials* (Ed.: H. Yersin), Wiley-VCH, Weinheim, **2007**, pp. 259–282; h) C.-M. Che, C.-C. Kwok, S.-W. Lai, A. F. Rausch, W. J. Finkenzeller, N. Zhu, H. Yersin, *Chem. Eur. J.* **2010**, *16*, 233–247.
- [3] a) C. Adachi, M. A. Baldo, M. E. Thompson, S. R. Forrest, *J. Appl. Phys.* **2001**, *90*, 5048–5051; b) M. Ikai, S. Tokito, Y. Sakamoto, T. Suzuki, Y. Taga, *Appl. Phys. Lett.* **2001**, *79*, 156–158; c) S. Tokito, T. Iijima, Y. Suzuri, H. Kita, T. Tsuzuki, F. Sato, *Appl. Phys. Lett.* **2003**, *83*, 569–571.
- [4] a) P. F. van Hutten, V. V. Krasnikov, G. Hadziioannou, *Acc. Chem. Res.* **1999**, *32*, 257–265; b) Z. I. Niazimbetova, A. Menon, M. E. Galvin, *Polym. Prepr.* **2003**, *44*, 659–660; c) I. F. Perepichka, D. F. Perepichka, H. Meng, F. Wudl, *Adv. Mater.* **2005**, *17*, 2281–2305; d) J. M. Hancock, A. P. Gifford, R. D. Champion, S. A. Jenekhe, *Macromolecules* **2008**, *41*, 3588–3597.
- [5] a) D. A. Pardo, G. E. Jabbour, N. Peyghambarian, *Adv. Mater.* **2000**, *12*, 1249–1252; b) H. Becker, H. Spreitzer, W. Kreuder, E. Kluge, H. Vestweber, H. Schenk, K. Treacher, *Synth. Met.* **2001**, *122*, 105–110; c) B.-J. de Gans, P. C. Duineveld, U. S. Schubert, *Adv. Mater.* **2004**, *16*, 203–213; d) F. So, B. Krummacker, M. K. Mathai, D. Poplavskyy, S. A. Choulis, V.-E. Choong, *J. Appl. Phys.* **2007**, *102*, 091101.
- [6] K. Watanabe, D. Kumaki, T. Tsuzuki, E. Tokunaga, S. Tokito, *J. Photopolym. Sci. Technol.* **2007**, *20*, 39–42.
- [7] a) J.-H. Jou, M.-C. Sun, H.-H. Chou, C.-H. Li, *Appl. Phys. Lett.* **2005**, *87*, 043508–043508; b) X. Yang, D. Neher, D. Hertel, T. K. Däubler, *Adv. Mater.* **2004**, *16*, 161–166; c) X. Yang, D. C. Müller, D. Neher, K. Meerholz, *Adv. Mater.* **2006**, *18*, 948–954; d) X. H. Yang, D. Neher, *Appl. Phys. Lett.* **2004**, *84*, 2476–2478.
- [8] a) A. L. Kanibolotsky, R. Berridge, P. J. Skabara, I. F. Perepichka, D. D. C. Bradley, M. Koeberg, *J. Am. Chem. Soc.* **2004**, *126*, 13695–13702; b) Q.-D. Liu, J. Lu, J. Ding, M. Day, Y. Tao, P. Barrios, J. Stupak, K. Chan, J. Li, Y. Chi, *Adv. Funct. Mater.* **2007**, *17*, 1028–1036; c) W.-Y. Lai, Q.-Y. He, R. Zhu, Q.-Q. Chen, W. Huang, *Adv. Funct. Mater.* **2008**, *18*, 265–276; d) Q. Xin, X.-T. Tao, F.-Z. Wang, J.-L. Sun, D.-C. Zou, F.-J. Wang, H.-J. Liu, Z. Liu, Y. Ren, M.-H. Jiang, *Org. Electron.* **2008**, *9*, 1076–1086.
- [9] a) X. Zeng, M. Tavasli, I. F. Perepichka, A. S. Batsanov, M. R. Bryce, C.-J. Chiang, C. Rothe, A. P. Monkman, *Chem. Eur. J.* **2008**, *14*, 933–943; b) M. Tavasli, S. Bettington, I. F. Perepichka, A. S. Batsanov, M. R. Bryce, C. Rothe, A. P. Monkman, *Eur. J. Inorg. Chem.* **2007**, 4808–4814; c) B. Liang, L. Wang, Y. Xu, H. Shi, Y. Cao, *Adv. Funct. Mater.* **2007**, *17*, 3580–3589; d) M. Tavasli, S. Bettington, M. R. Bryce, H. A. Al Attar, F. B. Dias, S. King, A. P. Monkman, *J. Mater. Chem.* **2005**, *15*, 4963–4970; e) A. Tsuboyama, H. Iwawaki, M. Furugori, T. Mukaide, J. Kamatani, S. Igawa, T. Moriyama, S. Miura, T. Takiguchi, S. Okada, M. Hoshino, K. Ueno, *J. Am. Chem. Soc.* **2003**, *125*, 12971–12979; f) J. C. Ostrowski, M. R. Robinson, A. J. Heeger, G. C. Bazan, *Chem. Commun.* **2002**, 784–785.
- [10] a) T.-C. Cheung, K.-K. Cheung, S.-M. Peng, C.-M. Che, *J. Chem. Soc. Dalton Trans.* **1996**, 1645–1651; b) W. Staroske, M. Pfeiffer, K. Leo, M. Hoffmann, *Phys. Rev. Lett.* **2007**, *98*, 197402; c) B.-P. Yan, C. C. C. Cheung, S. C. F. Kui, H.-F. Xiang, V. A. L. Roy, S.-J. Xu, C.-M. Che, *Adv. Mater.* **2007**, *19*, 3599–3603; d) M. Cocchi, D. Virgili, V. Fattori, D. L. Rochester, J. A. G. Williams, *Adv. Funct. Mater.* **2007**, *17*, 285–289; e) L. Murphy, J. A. G. Williams, *Top Organomet. Chem.* **2010**, *28*, 75–111.
- [11] a) S. C. F. Kui, I. H. T. Sham, C. C. C. Cheung, C.-W. Ma, B. Yan, N. Zhu, C.-M. Che, W.-F. Fu, *Chem. Eur. J.* **2007**, *13*, 417–435; b) G. S.-M. Tong, C.-M. Che, *Chem. Eur. J.* **2009**, *15*, 7225–7237.
- [12] a) P. Shao, Y. Li, J. Yi, T. M. Pritchett, W. Sun, *Inorg. Chem.* **2010**, *49*, 4507–4517; b) G.-J. Zhou, Q. Wang, W.-Y. Wong, D. Ma, L. Wang, Z. Lin, *J. Mater. Chem.* **2009**, *19*, 1872–1883; c) G.-J. Zhou, W.-Y. Wong, B. Yao, Z. Xie, L. Wang, *J. Mater. Chem.* **2008**, *18*, 1799–1809; d) G.-J. Zhou, X.-Z. Wang, W.-Y. Wong, X.-M. Yu, H.-S. Kwok, Z. Lin, *J. Organomet. Chem.* **2007**, *692*, 3461–3473.
- [13] C. M. Che, C. F. Kui, C. C. Kwok, US non-provisional patent application No. 12/485,388, **2009**.
- [14] J. Pommerehne, H. Vestweber, W. Guss, R. F. Mahrt, H. Bässler, M. Porsch, J. Daub, *Adv. Mater.* **1995**, *7*, 551–554.
- [15] C.-C. Kwok, H. M. Y. Ngai, S.-C. Chan, I. H. T. Sham, C.-M. Che, N. Zhu, *Inorg. Chem.* **2005**, *44*, 4442–4444.
- [16] CCDC-776826 (**2**), 774058 (**3a**) and 776825 (**3c**) contain the supplementary crystallographic data for this paper. These data can be obtained free of charge from The Cambridge Crystallographic Data Centre via www.ccdc.cam.ac.uk/data_request/cif.
- [17] S. Lamansky, P. I. Djurovich, F. Abdel-Razzaq, S. Garon, D. L. Murphy, M. E. Thompson, *J. Appl. Phys.* **2002**, *92*, 1570–1575.

Received: June 4, 2010

Published online: October 19, 2010